Neuroscience 129 (2004) 85–92

PERSISTENT SUBTHRESHOLD VOLTAGE-DEPENDENT CATION SINGLE CHANNELS IN SUPRACHIASMATIC NUCLEUS NEURONS

N. I. KONONENKO,[a] I. MEDINA[b] AND F. E. DUDEK[a]*

[a]*Department of Biomedical Sciences, Section of Anatomy and Neurobiology, Colorado State University, Fort Collins, CO 80523, USA*

[b]*INMED, INSERM U 29, Marseille, France*

Abstract—The hypothalamic suprachiasmatic nucleus (SCN) contains the primary circadian pacemaker in mammals, and transmits circadian signals by diurnal modulation of neuronal firing frequency. The ionic mechanisms underlying the circadian regulation of firing frequency are unknown, but may involve changes in membrane potential and voltage-gated ion channels. Here we describe novel tetrodotoxin- and nifedipine-resistant subthreshold, voltage-dependent cation (SVC) channels that are active at resting potential of SCN neurons and increase their open probability (P_o) with membrane depolarization. The increased P_o reflects changes in the kinetics of the slow component of the channel closed-time, but not the channel open-time or fast closed-time. This study provides a background for investigation of the possible role of SVC channels in regulation of circadian oscillations of membrane excitability in SCN neurons.

Key words: SCN, circadian rhythm, spontaneous activity, electrical firing, regulation, non-selective channel.

Circadian oscillations of electrical activity by suprachiasmatic nucleus (SCN) neurons (Reppert and Weaver, 2002) are modulated by a transcription/translation mechanism and play a pivotal role in circadian behavior of mammals. Circadian oscillations of electrical activity are present at the cell level, even for isolated SCN neurons (Welsh et al., 1995; Honma et al., 1998). Although voltage-gated calcium channels (VGCC) and sodium channels (VGSC) are important for generation of spike activity of SCN neurons (Pennartz et al., 1997, 2002; Kononenko et al., 2004), neither the ionic mechanism of spontaneous activity nor the target for the cytoplasmic circadian modulation of electrical firing of SCN neurons has been definitively identified. The interesting feature of spontaneously active SCN neurons is that, after inhibition of both VGSC and VGCC with tetrodotoxin (TTX) and nifedipine, they still exhibit significantly different time-averaged membrane resting potential and input resistance during the day as compared with the night (Pennartz et al., 2002), suggesting involvement of other ion channels/transporters in setting of the resting membrane potential. Conventional whole cell recordings may not be useful for studies of the ion conductances that determine the membrane potential, because circadian rhythmicity in firing rate may not be detectable in whole cell recordings, except during the first few minutes after membrane rupture (Schaap et al., 1999; see also van den Top et al., 2001). To prevent the hypothesized rundown of currents responsible for circadian modulation of activity, perforated-patch recordings have been performed (de Jeu et al., 1998; van den Top et al., 2001; Shimura et al., 2002; Teshima et al., 2003). An alternative approach to studying the mechanisms of spontaneous firing is the use of cell-attached recordings, whereby the firing pattern can be studied along with single-channel activity. Here we have analyzed single-channel currents in isolated SCN neurons using non-invasive cell-attached patch-clamp recording. We have found that the majority of neurons express at resting potential cation single-channel currents whose activity depends on membrane potential. Thus, these channels might be involved in processes related to spontaneous electrical firing in SCN neurons.

*Corresponding author. Tel: +1-970-491-2942; fax: +1-970-491-2623.
E-mail address: ed.dudek@colostate.edu (F. E. Dudek).

Abbreviations: ACSF, artificial cerebrospinal fluid; SCN, suprachiasmatic nucleus; SVC, subthreshold voltage-dependent cation; TRP, transient–receptor–potential; TTX, tetrodotoxin; VGCC, voltage-gated calcium channel; VGSC, voltage-gated sodium channel; τ_{sc}, slow component of the channel closed-time.

EXPERIMENTAL PROCEDURES

Preparation of isolated neurons

The procedure for preparation of acutely isolated Sprague–Dawley rat SCN neurons is described in Kononenko et al. (2004). Neurons were incubated at least 72 h prior to electrophysiological recordings that were conducted during the subsequent 4 days. All rats (n=78) used for cultures were maintained in a light/dark cycle (light on 6:00 a.m.; light off 6:00 p.m.), cultures were prepared between 9:00 and 11:00 a.m. and experiments were performed from 11:00 a.m. to 4:00 p.m. The animal protocols were approved by the Animal Care and Use Committee at Colorado State University, and they were in accordance with the NIH Guide on the Humane Treatment of Experimental Animals and minimized the number and suffering of animals.

Electrical recording

Artificial cerebrospinal fluid (ACSF) containing (in mM) 124 NaCl, 3 KCl, 2.5 $CaCl_2$, 2 $MgSO_4$, 1.25 NaH_2PO_4, 26 $NaHCO_3$, and 10 dextrose, continuously aerated with 95% O_2 and 5% CO_2 to a final pH of 7.4, osmolarity 300 mOsm was used as an external bath solution. Pipettes for cell-attached recordings were prepared from glass microcapillaries (Garner Glass Co.) and coated to near the tip with Sylgard elastomer (Dow Corning Corp.). Two basic solutions were used in the patch pipettes for recordings: solution 1 or Na^+-containing solution (in mM): 135 NaCl, 10 EGTA, 1 EDTA, 10 HEPES (pH 7.0–7.1 with NaOH; final Na^+ concentration was 160), osmolarity 290 mOsm, and solution 2 or K^+-containing solution (in mM): 135 KCl, 10 EGTA, 1 EDTA, 10 HEPES (pH 7.0–7.1 with KOH; final K^+ concentration was 148), osmolarity 285 mOsm. In many patches, before subsequent whole cell recording (results not shown in current paper), cell-attached record-

0306-4522/04$30.00+0.00
doi:10.1016/j.neuroscience.2004.06.080

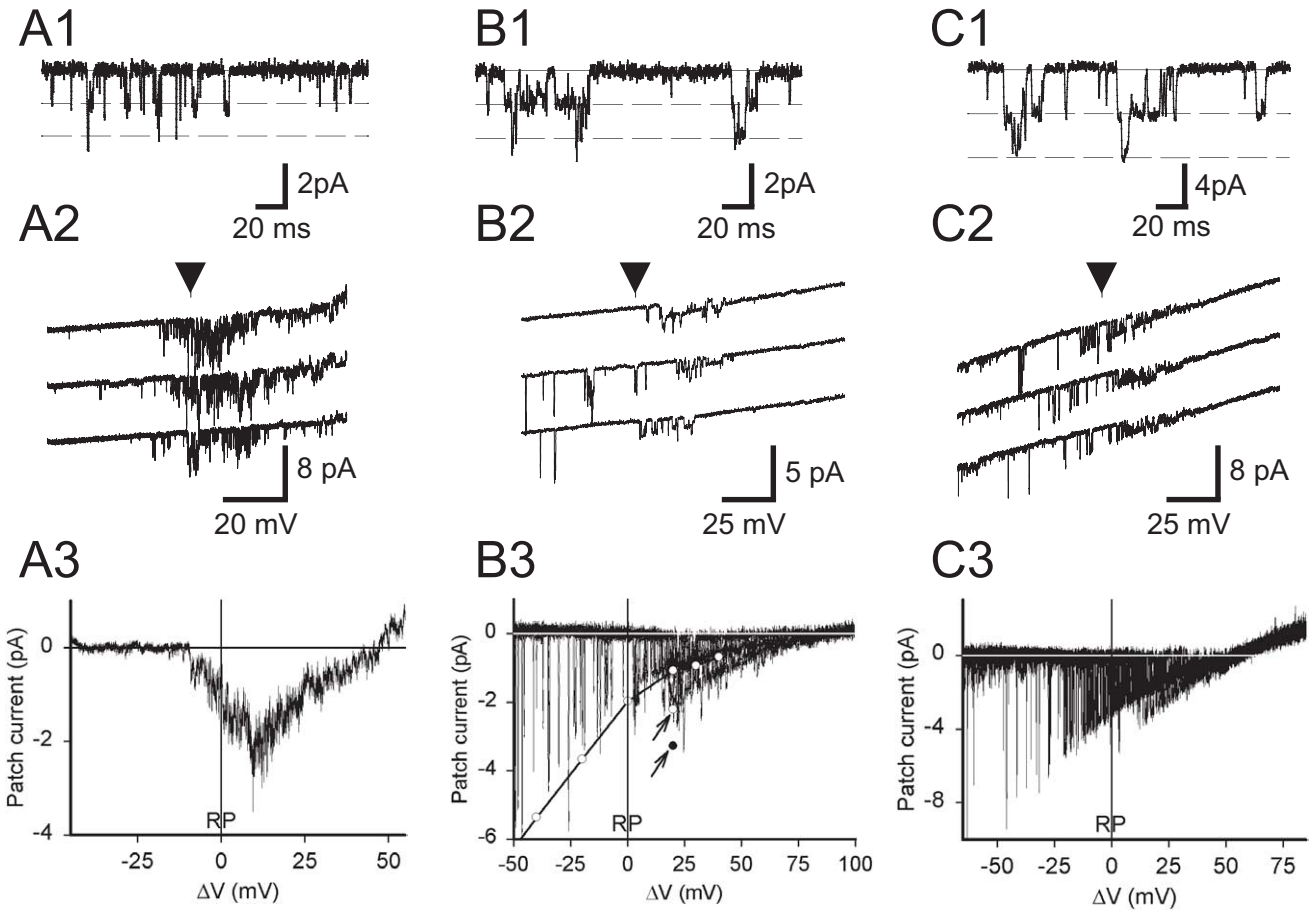

Fig. 1. Persistent voltage-dependent single channels of isolated SCN neurons with NaCl-, KCl- and K-gluconate-filled patch pipettes (A, B and C, respectively). Single-channel activity at resting potential (A1, B1 and C1) and three consecutive ramp (100 mV/s) I–V relationships (A2–C2) revealing voltage-activated channels. Actually, at resting potential (A1–C1), a double level of single-channel currents was rare, and corresponding fragments were chosen to demonstrate this point. Triangles show bath pipette potential. (A3) Ten average consecutive I–V relationships. Linear gigaseal leakage (47.6 GΩ) was subtracted. (B3) Eight applied ramp patch I–V relationships demonstrate increased open probability with depolarization of patch membrane. Linear gigaseal leakage (46.5 GΩ) was subtracted. I–V relationship (open circles, taken from Fig. 2, B3) was constructed from steady-state recordings for the same patch. Circles marked by arrows show second (open circle) and third (closed circle) levels of single-channel currents. (C3) Seven applied patch I–V relationships demonstrate increased open probability with depolarization of patch membrane. Slight non-linear gigaseal leakage (approximately 9.4 GΩ) was fitted by parabola and subtracted.

ings were obtained with a pipette containing K-gluconate solution (solution 3), mimicking intracellular content: 120 K^+ gluconate, 10 HEPES, 1 NaCl, 1 $MgCl_2$, 1 $CaCl_2$, 3 KOH (to pH 7.2–7.4), 5 EGTA, 2 Na_2ATP, osmolarity 255 mOsm (i.e. K^+-containing, low-Cl^- solution). Pipette resistance was 4–5 MΩ when filled with solution 1 or 2, and 7–8 MΩ with K-gluconate solution. The seal resistance ranged between 2 and 60 GΩ. A neuron was only used for one cell-attached recording.

During recording, the dish was superfused at 1.5–2.5 ml/min (18–20 °C). Offset potential was zeroed just before the electrode contacted the neuronal membrane. Single-channel currents were recorded with an Axopatch-1D patch-clamp amplifier (cutoff 2 kHz), digitally filtered at 0.5 kHz for ramp recording and not filtered for steady-state recording, sampled at 10 kHz, and analyzed with pClamp8 software (Axon Instruments). All voltage measurements were corrected off-line for the liquid-junction potential, which amounted to +5 mV for the NaCl-filled pipettes, 0 mV for KCl-filled pipettes, and −15 mV for the K-gluconate-filled ones. I–V relationships of patch membrane were constructed using both current and voltage digital recordings, and RP shows resting (bath) potential; positive ΔV means depolarization of patch membrane, while negative ΔV indicates hyperpolarization.

Analysis of single-channel properties

Open and closed states were defined as when current amplitudes were above or below, respectively, the 50% level. Kinetic components were determined from patches with one-level channel openings. Channel openings and closings of <0.3 ms were not analyzed. Mean single-channel current amplitudes were obtained as maximums of all-points histograms. In all figures (excluding Fig. 5), inward single-channel currents are shown as downward deflections (closed state, solid line; open state(s), dashed line(s)). Closed and open states correspond to the maximums of all-points histograms.

For estimation of the single-channel conductance, we used two different approaches. First, we measured conductance based on changes of the channel's amplitude during application of the ramp protocol. These results were then confirmed for each experimental condition using "all-points histogram analysis" of amplitudes of steady-state single-channel currents recorded at different membrane potentials as shown in Fig. 2. The value of the channel conductance was determined using regression fits of voltage-current relationships. Fig. 1B3 illustrates correspondence of the values of channel amplitudes obtained from all-points histogram

Table 1. The effect of 20 mV depolarization of patch membrane on the kinetic of single channels recorded using patch pipette filled with Na^+ (n=3) or K^+ (n=3 with KCl-filled pipette and n=3 with K-glu-filled pipette)[a]

Main ion in pipette and patch membrane potential		Open times		Closed times	
		Fast τ_{fo} (ms)	Slow τ_{so} (ms)	Fast τ_{fc} (ms)	Slow τ_{sc} (ms)
Na^+	0 mV	N/A	<0.5	0.83±0.10	13.37±0.13
	ΔV 20 mV	N/A	<0.5	0.96±0.05	5.23±0.55
K^+	0 mV	0.67±0.22	3.49±1.46	1.11±0.16	118±57*
	ΔV 20 mV	<0.5	3.76±0.88	1.00±0.19	51±25*

[a] Values are means±S.E.M. (n=3/6).

* Slow τ_{sc} of channels recorded using K^+- filled pipette showed strong initial variation from cell to cell. The paired comparison of this parameter yielded 2.49±0.17-fold decrease at 20 mV patch membrane depolarization.

plots with amplitudes recorded using ramp protocol. The reversal potential of channels under different experimental conditions was determined as the point of crossing of the voltage-current relationships fitting curve with zero-current axis. Data are presented as mean±S.E.M. For cross-correlation analysis between single-channel open probability and spontaneous action-potential firing, prior to application of the cross correlation, the low-frequency sampled open probability was upsampled to 10 kHz by inserting the corresponding number of zero datum points in-between each sample in the data.

Chemicals and drugs

All chemicals and drugs were obtained from Sigma, except TTX (Sigma and Alomone Laboratories). TTX was used as a 1 mM stock solution in distilled water, and then diluted to its final concentration in patch pipette solution. Stock solution (10 mM) of nifedipine was prepared in DMSO, and then diluted to its final concentration in patch pipette solution.

RESULTS

Voltage-dependence of single-channel currents

About 25% of cell-attached patches (98 out of approximately 370) exhibited single-channel currents that are characterized below and defined as subthreshold, voltage-dependent cation (SVC) channels. The prominent feature of these channels, which were active at resting potential, was their nonlinear voltage dependence. The remaining approximately 75% of the patches either did not show any single-channel activity or included other types of channels (n=approximately 95) with irregular kinetics and amplitudes or with voltage-independent channels. These channels were not studied further.

At resting membrane potential, SVC single-channel currents recorded with a pipette filled with Na-containing solution (n=28 patches) were inwardly directed (Fig. 1, A1) and had amplitudes ranging from values close to 0 pA to 2 pA in different patches (1.52±0.14 pA; n=10). Variability in the amplitude presumably reflected the differences in resting membrane potential of different SCN neurons that can occur even during the same circadian time (Teshima et al., 2003). In agreement with these data, resting potential varied from −85 to −40 mV in our experiments with whole cell recordings using K-gluconate-filled pipettes (n=96; not shown here) from isolated SCN neurons. Significant variation of single-channel amplitude (from value close to zero) may also be related to the small open-time of the single channels (<0.5 ms; see below and Table 1) with Na-filled patch pipette. Alteration of the patch membrane potential using applications of voltage ramps from −45 mV to +55 mV resulted in a clear change in the channel activity and amplitudes. At hyperpolarized potentials, the channel was silent, while depolarization of the patch membrane progressively increased the frequency of channel openings (Fig. 1, A2). The profile of the averaged cell-attached currents (Fig. 1, A3) exhibited a negative-resistance region on the current-voltage (I–V) relation of the patch membrane. Although a similar profile of voltage dependence was observed in all patches studied, the absolute value of voltage thresholds for channel openings as well as reversal potential values varied strongly from patch to patch. In 20 of 28 of patches, the channel was open at resting membrane potential and complete closing occurred after membrane hyperpolarization, whereas in the remaining eight patches, the channel was silent at resting potential and was activated during membrane depolarization. The threshold for the channel opening ranged between −25 mV and +10 mV compared with the resting potential.

A similar voltage-dependence of the channels (Fig. 1B) was observed when Na^+ in the patch pipette solution was replaced with K^+ (solution 2; n=32 patches); however, the kinetics and amplitude (3.79±0.32 pA; n=22) of the single-channel currents at resting membrane potential were different than in recordings with a Na^+-filled pipette (Fig. 1A1, B1; see also Figs. 2 and 3B, C).

The decrease of $[Cl^-]_i$ from 135 mM to 5 mM (substitution of 130 mM KCl with equiosmolar amount of K-gluconate; n=38 patches) had no detectable effect on single-channel current at resting potential (4.10±0.57 pA, n=12; P approximately 0.6) or on the voltage dependence (Fig. 1C), conductance or kinetic properties of single channels (see below). The SVC single-channel currents were also not affected by TTX (1 μM, n=8 patches) or nifedipine (10 μM, n=8 patches) in the patch-pipette solution.

Single-channel conductance

Fig. 2 shows the results of the analysis of single-channel conductances recorded with different pipette solutions. The conductance of channels recorded with Na^+ ions in the pipette estimated as slope of single-channel current amplitude (e.g. see Fig. 2, A3) was 55.2±5.1 pS (n=21). Unlike the case of Na^+ ions in patch pipette, the channel conductance measured when the patch pipette contained

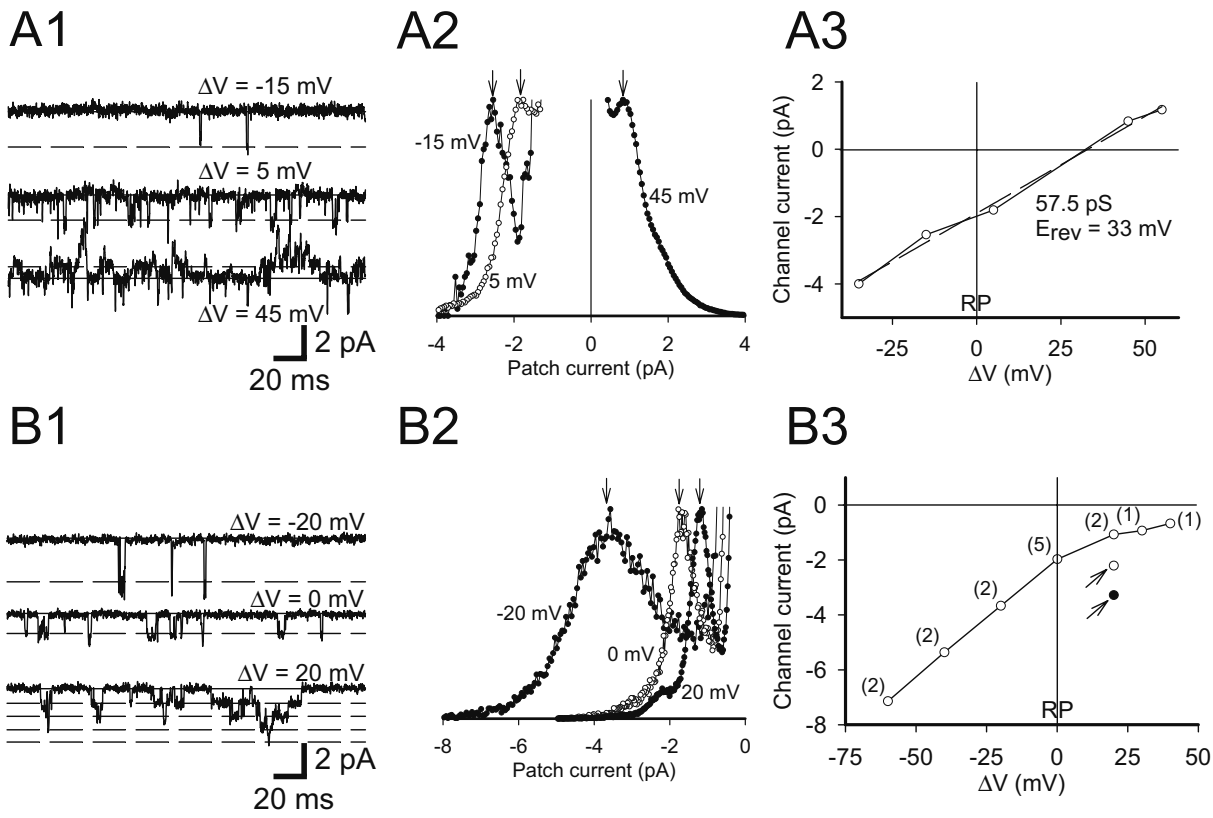

Fig. 2. Single-channel conductance with Na^+- and K^+-filled patch pipette (A and B, respectively). The left panels (A1 and B1) show examples of opening of single channels recorded at three different patch potentials (values near corresponding records). Solid and dashed lines show closed and open levels, respectively, in accordance with maximums of all-points histograms (middle panels, A2 and B2). Amplitudes of peaks corresponding to the open states of single channel in A2 and B2 (shown by arrows) were normalized. The right panels (A3 and B3) show the maximums of open-points amplitude histogram (A2 and B2) plotted against ΔV of patch membrane. Figures within brackets in B3 are the number of analyzed fragments of recordings from the same patch. Error bars are less than symbol. Regression fitting in A3 for linear function estimated conductance of single channel as 57.5 pS and E_{rev} for current through this channel as 33 mV positive to the resting potential. Regression fitting in B3 for linear function estimated conductance of single channel and E_{rev} for current through this channel below resting potential as 85.9 pS and 22.8 mV and above of resting potential as 35.0 pS and 55.3 mV. In B3, circles marked by arrows show second (open circle) and third (closed circle) levels of single-channel currents.

K^+ ions (solution 2) was non-linear within the studied range of potentials (Fig. 2, B3; see also ramp recordings on Fig. 1, B3 and C3). We did not find statistically significant differences in studied parameters between single channels with KCl- and K-gluconate-filled pipettes (n=32 and 38 patches, respectively) using both ramp and steady-state protocols, and therefore these results were combined in the sections below. In the range of potentials negative of resting potential, single-channel conductance was 85.1±6.4 (n=23). In the range of positive potentials, it was 38.8±4.1 pS (n=23). The average reversal potential of currents recorded with Na^+ and K^+ in the pipette was greater for K-filled pipettes: 42.7±3.6 mV (n=21) and 63.8±3.6 mV (n=23) positive to the resting potential, respectively.

Voltage-dependence of open probability

To estimate the voltage-dependence of the open probability, P_o–V_m, of the channels, as a possible basis for the negative-resistance region of the patch membrane (Fig. 1, A3), we used squares of corresponding open-points amplitude histograms of single-channel activity with K-filled pipettes, because of the higher single-channel amplitude (compared with Na^+-filled pipette) and longer open time constant of the single channel. Fig. 3A illustrates P_o–V_m relationships for different patches (n=5). When averaged and fitted by the Boltzmann equation, this relationship yielded a half-activation potential of 23.5 mV positive to the resting potential and a slope factor 9.4 mV. The P_o of single-channel activity at bath patch potential varied strongly from cell to cell, and ranged from 0.03–0.7 with K^+-filled pipettes (n=14).

Kinetic properties of single channels

To characterize the kinetic components responsible for the voltage-dependence of open probability, we analyzed the steady-state kinetics of the single channel in patches showing a single level of channel opening at different potentials. The open and slow closed kinetics for single channels with K^+-filled pipettes were significantly slower than with Na^+-filled pipettes. The τ_{sc} with K^+-filled pipettes, in contrast to the Na^+-filled one, varied in different neurons from 12 to 360 ms. Using Na- and K-filled pipettes, the 20 mV depolarization of patch membrane in-

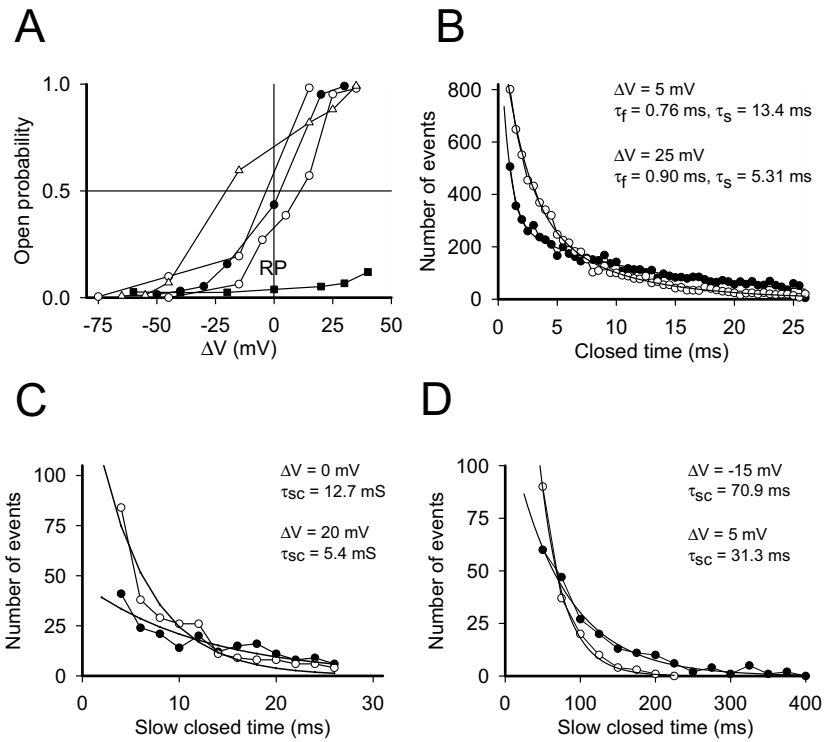

Fig. 3. Open probability, P_o, and closed-time constant. (A) P_o of channel in five patches plotted against ΔV of patch membrane. Amplitude histograms at different patch membrane potentials fitted by the sum of two, three or four Gaussians were used, and P_o was obtained from the areas under the fitted curves as $(1-S_C/(S_C+\Sigma S_O))$. Experiments were conducted with KCl-filled pipettes (closed circles) and K-gluconate-filled ones (open circles). (B) Fast and slow closed-time distribution for the single-channel activity recorded with Na^+-filled pipette from Fig. 1A at close to resting potential (closed circles) and at 20 mV depolarization (open circles) at potentials 5 and 25 mV, respectively. Distributions were fitted by two-exponential density (smooth line). (C) Slow closed-time distributions for the single-channel activity recorded with K^+-filled pipette at resting potential (closed circles) and 20 mV depolarization (open circles). (D) Slow closed-time distributions for the single-channel activity recorded with K-gluconate-filled pipette at ΔV = −15 mV (closed circles) and 20 mV depolarization (open circles).

duced a significant (one-tailed paired t-test, $P<0.05$, $n=3/6$) decrease of the exponentials describing slow component of the channel closed-time (τ_{sc}), whereas the kinetics of the channel open-time and fast closed-time were not modified (Fig. 3B–D). The effect of depolarization of the patch membrane on mean kinetic components of the single channel for Na^+- and K^+-filled pipettes is shown in Table 1.

Spontaneous modulation of open probability

In most patches, we observed spontaneous transient increases in the open probability at resting potential during prolonged recordings of single-channel steady-state activity (Fig. 4A). In the analyzed cases ($n=10$), these transient bursts of P_o were due mainly to changes of τ_{sc} (Fig. 4B), whereas channel fast closed-time and open-time parame-

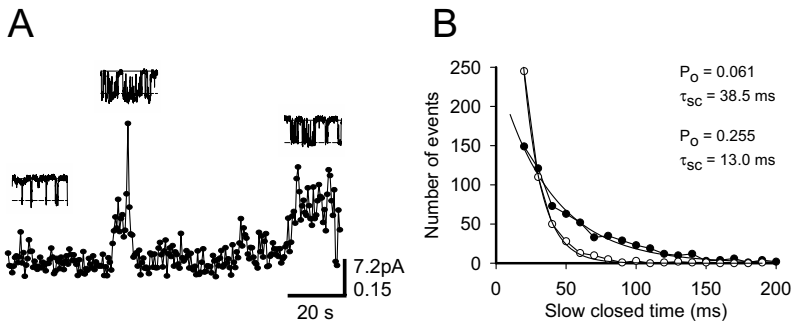

Fig. 4. (A) Spontaneous transient increase of open probability of single-channel activity at resting potential. Recording was obtained with K-gluconate-filled pipette. Entire record is 120 s. Lowest points on the plot correspond to $P_o=0$. The P_o was calculated over a 500-ms time interval. Insets represent 200-ms fragments of single-channel activity from 0 s ($P_o=0.061$ in interval 0–38 s), 43rd s ($P_o=0.650$ in interval 42.8–43.8 s) and 110th s ($P_o=0.255$ in interval 100–120 s). (B) Slow closed-time distributions for single-channel activity during spontaneous transient modulation of open probability. Data are taken from A. Closed circles present interval 0–38 s with $P_o=0.061$; open circles present interval 100–120 s with $P_o=0.255$.

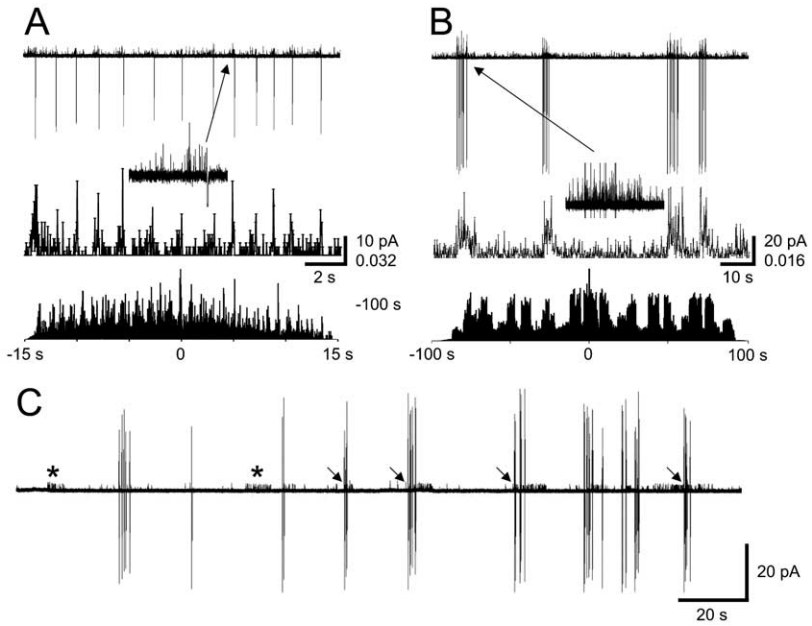

Fig. 5. Spontaneous transient increase in P_o of single-channel activity at resting potential correlated with repetitive (A) or bursting (B) action-potential firing. Recordings were obtained with a Na^+-filled pipette. Upper record, cell-attached single-channel and action-potential activity; here, inward single-channel currents are shown as upward deflections while action-potential currents are shown as downward deflections. Middle record, P_o of single-channel activity calculated over a 20-ms (A) and a 100-ms (B) time interval. For calculation of the P_o, trace was analyzed manually; events corresponding to spike currents were disregarded. Lowest points on the plot correspond to $P_o=0$. Insets, single-channel and action-potential activity recorded at expanded time and amplitude scale; action potentials are truncated. Lower record, cross-correlation between action-potential activity and single-channel P_o during periods of recording (15 s for A and 100 s for B). (C) Spontaneous transient increase in P_o of single-channel activity at resting potential only partially correlated with spontaneous action-potential firing. Recording was obtained with a KCl-filled pipette. Arrows show correlation between single-channel activity and action-potential firing while asterisks show single-channel current bursts without action-potential generation.

ters were unmodified (not shown). Thus, changes similar to those induced by changes of the membrane potential took place during spontaneous bursts of channel activity.

In some patches ($n=8$), it was possible to observe simultaneously SVC single-channel currents and spike currents, which reflect spontaneous action-potential firing. Under these conditions, single spike currents (Fig. 5A) or bursts of spike currents (Fig. 5B) coincided with periods of increased channel activity and, correspondingly, its P_o. The lower recordings of Fig. 5A, B show the cross-correlation histograms of the action-potential activity and single-channel P_o. These histograms have distinct peaks at zero time, indicating correlated activation of single channel(s) and generation of action potentials in acutely isolated SCN neurons.

In many other patches ($n>30$), however, this obvious correlation was obscured by the presence of numerous action potentials that did not correlate with single-channel P_o or by bursts of single-channel currents that were not accompanied by action-potential firing (Fig. 5C). Analysis of single-channel kinetics revealed that the increase of P_o was due to a decrease of τ_{sc} of single-channel events ($n=5$) similar to those demonstrated in Fig. 4B. These observations indicate that the above-described SVC channels are likely to be of physiological relevance.

DISCUSSION

Here we describe properties of single-channel currents, which we defined as SVC channels that are highly represented in SCN neurons under resting conditions. One prominent feature of these channels is that they are partially open at resting membrane potential, and under physiological conditions this provides a depolarizing force to the neuron. The probability of channel opening increases progressively with membrane depolarization. A simple estimation shows that an SCN neuron with a diameter of approximately 10 μm (membrane surface approximately 300 μm^2) possesses at least 75 channels. Simultaneous opening of these channels could provide a conductance equal to 3–4 nS near resting potential. Given that the average conductance measured at resting conditions using whole cell recording of isolated SCN neurons is approximately 0.3 nS (Kononenko et al., 2004), and for SCN neurons in slice preparations it is approximately 1 nS (Pennartz et al., 1998), the modulation of SVC channel opening might have an important effect on the level of resting membrane potential.

Analysis of the properties of the single-channel currents recorded using patch pipettes filled with Na^+-, K^+-, Cl^-- and gluconate$^-$-containing solutions suggests that SVC channels are selective for cations. Although the kinetic properties and conductances of the channel recorded with Na^+ and K^+ were different, all other experimental data indicate that single-channel currents flow through the same kind of channels in both cases. Indeed, both SVC_{Na} and SVC_K channels were active at resting potential and showed a strong voltage-dependence of P_o that was primarily due to voltage-dependence of τ_{sc}. The reversal potentials of SVC_{Na} were 20 mV

more negative than those of SVC_K single-channel currents measured under conditions close to symmetrical. In SCN neurons, the reversal potential estimated using perforated patches was +41 mV for Na^+ (Huang, 1993) and −107 mV for K^+ (Teshima et al., 2003). Thus, under asymmetrical cation conditions (Na^+_o/K^+_i), potassium-selective channels should show a strong (approximately −100 mV) shift of the reversal potential toward negative potentials, whereas sodium-selective channels should result in a shift to more positive reversal potentials. The slight negative shift of the reversal potential in our experiments suggests that the recorded channels are cation-selective, probably with a higher permeability for K^+ than for Na^+. At resting membrane potential, channel opening provides a depolarizing force, and this force progressively decreases with membrane depolarization and could even be reversed after membrane depolarization to values more positive than −20 mV. As one can see from Fig. 1A3–C3, hyperpolarization of patch membrane more effectively suppressed spontaneous opening of SVC_{Na} than SVC_K channels. A possible mechanism that might explain this observation could be that the open time of SVC_{Na} channels is approximately 20-fold shorter that those for SVC_K channels (Table 1). Under the conditions when hyperpolarization produced a strong increase of the closed time of SVC channels, such events could be rather rare for SVC_{Na} channels in comparison with SVC_K channels (compare, for example, upper recordings in Fig. 2A1, B1). Further, although we did not find a significant effect of depolarization on open time of SVC channels, we cannot exclude that hyperpolarization may decrease it, and this could also contribute in strong suppression of SVC_{Na} channels at hyperpolarization.

Voltage-dependent cation currents have been studied previously; for example, these currents have been proposed to have an important role in spontaneous firing of rat neocortical neurons (Alzheimer, 1994). Expression of hippocampal transient–receptor–potential (TRP) channels in HEK cells resulted in a non-selective cation channel exhibiting a voltage-dependence (Strübing et al., 2001). Open probability of voltage-dependent TRP cation channels was increased approximately 90% after dialysis of cells with GTP[γ-S], while the single-channel current amplitude remained unchanged, which suggested the participation of G proteins in up-regulation of these channels (Hambrecht et al., 2000). Also, rod non-selective cAMP-gated channels showed a sizeable voltage-dependence of P_o, exhibiting prolonged periods in the open state at positive potentials and only brief opening at negative potentials (Bonigk et al., 1999). Interestingly, this voltage dependence was more pronounced at low (1 μM) compared with high (3 μM) cAMP concentrations. From another perspective, 40-pS cation channels (not voltage-activated) that are permeable to Ca^{2+} and active in the night but not during the day have been described in pineal cells (D'Souza and Dryer, 1996), and protein synthesis was required for diurnal regulation of their activity (D'Souza and Dryer, 1997).

In addition to the voltage dependence, one of the distinctive features of the SVC channel in SCN neurons is its short open-time (τ_o), which is below the frequency resolution for recordings using Na^+-containing pipettes and a few milliseconds for recordings using K^+-containing pipette. A similar dependence of the apparent mean open time on the permeant ion, K^+ vs. Na^+, has been reported for cyclic nucleotide-gated channels (Holmgren, 2003; see also this paper for references for other types of channels). The estimated values of τ_o are indicative since, in addition to the limit induced by the frequency cutoff, the presence of multiple channels in one patch might induce an additional error. We did not find a statistically significant effect of patch membrane depolarization on τ_o for either SVC_{Na} or SVC_K channels. By contrast, in every patch, depolarization of the patch membrane by 20 mV produced approximately 2.5-fold decrease of the time constant describing the slow closed state of the SVC channels. Thus, τ_{sc} was the only parameter sensitive to membrane potential. Further studies using isolated patches are required, however, to determine the exact biophysical properties of SVC channels.

Interestingly, in most experiments with long-term steady-state recording of SVC channels using both K^+-filled (Figs. 4A, 5C) or Na^+-filled pipette (Fig. 5A, B), we have observed a transient increase of open probability at resting potential. In addition to the patch membrane depolarization imposed via the recording pipette, spontaneous changes of open probability were also accompanied by changes of only τ_{sc}. This suggests an active role of SVC channels in the setting of the membrane conductance of SNC neurons under resting conditions, but the mechanisms regulating SVC channel activity remain unclear. Multiple scenarios could be proposed to describe their functional role: 1) the channels are metabolically dependent, and their regulation causes changes in resting potential sufficient for maintenance of different rates of neuron firing (pacemaker channels); 2) channel activity depends exclusively on the level of the membrane potential. In this case, the role of the channels would be limited to the amplification of the oscillations of membrane potential. Slight membrane depolarization via modification of other channels or ion transporters would lead to an increase of SVC currents and facilitation of neuronal firing, and vice versa; and, 3) it is possible that SVC channels are not implicated in circadian oscillations, but simply participate in generation of neuronal firing by inducing membrane depolarization that leads to spike initiation.

We have not found an obvious relationship between SVC single-channel currents and the whole cell currents in SCN neurons that have been described by others (Huang, 1993; Walsh et al., 1995; de Jeu and Pennartz, 1997; Teshima et al., 2003). In our experiments, all recordings were carried out with Ca^{2+}-free solution in the patch pipette because it dramatically improved gigaseal. Experiments with ACSF in pipette should also be done. Thus, we cannot exclude completely that the SVC channels described here have selective properties similar to cyclic nucleotide-gated channels (i.e. Ca^{2+}-permeable, nonselective cation channels that conduct mixed cation currents, which cannot be recorded in ACSF because of rapid blocking and unblocking of the channel by Ca^{2+}, thus making the opening events too brief to resolve; see, for example, Dzeja et al., 1999). The role of external Ca^{2+} (i.e. in pipette

solution) in the function of SVC channels could be important, especially in the light of data demonstrating circadian regulation of cyclic GMP-protein kinase G in SCN (Tischkau et al., 2003) and cyclic nucleotide-gated channels in chick cones (Ko et al., 2001, 2003, 2004), and further experiments are needed to investigate this issue.

An interesting observation is that in many cases spontaneous modulation of single-channel activity appeared to be directly correlated with spontaneous electrical firing (Fig. 5), although a cause-effect relation between these electrical events is lacking. At least two possibilities could be suggested. First, a transient activation of SVC channels both under and outside of the patch pipette from a putative cytoplasmic source evokes depolarization of the outside membrane (in reference to patch membrane) and action-potential generation. Second, a mutual cytoplasmic source produces depolarization of the neuronal membrane and, independently, activation of SVC channels and action-potential firing. Subsequent experiments with appropriate SVC channel blockers should distinguish these possible scenarios.

Concluding remarks

This work provides information concerning the properties of novel single-channels, which may be highly represented in SCN neurons. Under resting conditions, activation of these channels could provide an important driving force that leads to neuron depolarization. Taking into account that the main role of SCN neurons is circadian regulation of neuronal firing, and that the mechanisms of this regulation are unknown, future studies of the pharmacological and biophysical properties of these channels—as well as their functional significance—might be beneficial for understanding the mechanisms of circadian oscillations.

Acknowledgments—This research was supported by MH59995. The critical comments of anonymous referees leading to substantial improvement of the paper are greatly acknowledged.

REFERENCES

Alzheimer C (1994) A novel voltage-dependent cation current in rat neocortical neurones. J Physiol 479:199–205.

Bonigk W, Bradley J, Muller F, Sesti F, Boekhoff I, Ronnett GV, Kaupp UB, Frings S (1999) The native rat olfactory cyclic nucleotide-gated channel is composed of three distinct subunits. J Neurosci 19: 5332–5347.

de Jeu MT, Pennartz CM (1997) Functional characterization of the H-current in SCN neurons in subjective day and night: a whole-cell patch-clamp study in acutely prepared brain slices. Brain Res 767:72–80.

de Jeu M, Hermes M, Pennartz C (1998) Circadian modulation of membrane properties in slices of rat suprachiasmatic nucleus. Neuroreport 9:3725–3729.

D'Souza T, Dryer SE (1996) A cationic channel regulated by a vertebrate intrinsic circadian oscillator. Nature 382:165–167.

D'Souza T, Dryer SE (1997) Elevated nighttime activity of chick pineal ILOT channels requires protein synthesis. Biol Signals 6:212–216.

Dzeja C, Hagen V, Kaupp UB, Frings S (1999) Ca^{2+} permeation in cyclic nucleotide-gated channels. EMBO J 18:131–144.

Hambrecht J, Zimmer S, Flockerzi V, Cavalie A (2000) Single-channel currents through transient-receptor-potential-like (TRPL) channels. Pflugers Arch 440:418–426.

Holmgren M (2003) Influence of permeant ions on gating in cyclic nucleotide-gated channels. J Gen Physiol 121:61–72.

Honma S, Shirakawa T, Katsuno Y, Namihira M, Honma K (1998) Circadian periods of single suprachiasmatic neurons in rats. Neurosci Lett 250:157–160.

Huang R-H (1993) Sodium and calcium currents in acutely dissociated neurons from rat suprachiasmatic nucleus. J Neurophysiol 70:1692–1703.

Ko GY, Ko ML, Dryer SE (2001) Circadian regulation of cGMP-gated cationic channels of chick retinal cones: Erk MAP kinase and Ca^{2+}/calmodulin-dependent protein kinase II. Neuron 29:255–266.

Ko GY, Ko ML, Dryer SE (2003) Circadian phase-dependent modulation of cGMP-gated channels of cone photoreceptors by dopamine and D2 agonist. J Neurosci 23:3145–3153.

Ko GY, Ko ML, Dryer SE (2004) Circadian regulation of cGMP-gated channels of vertebrate cone photoreceptors: role of cAMP and Ras. J Neurosci 24:1296–1304.

Kononenko NI, Shao LR, Dudek FE (2004) Riluzole-sensitive slowly inactivating sodium current in rat suprachiasmatic nucleus neurons. J Neurophysiol 91:710–718.

Pennartz CM, Bierlaagh MA, Geurtsen AM (1997) Cellular mechanisms underlying spontaneous firing in rat suprachiasmatic nucleus: involvement of a slowly inactivating component of sodium current. J Neurophysiol 78:1811–1825.

Pennartz CM, de Jeu MT, Geurtsen AM, Sluiter AA, Hermes ML (1998) Electrophysiological and morphological heterogeneity of neurons in slices of rat suprachiasmatic nucleus. J Physiol 506:775–793.

Pennartz CM, de Jeu MT, Bos NP, Schaap J, Geurtsen AM (2002) Diurnal modulation of pacemaker potentials and calcium current in the mammalian circadian clock. Nature 416:286–290.

Reppert SM, Weaver DR (2002) Coordination of circadian timing in mammals. Nature 418:935–941.

Schaap J, Bos NP, de Jeu MT, Geurtsen AM, Meijer JH, Pennartz CM (1999) Neurons of the rat suprachiasmatic nucleus show a circadian rhythm in membrane properties that is lost during prolonged whole cell recording. Brain Res 815:154–166.

Shimura M, Akaike N, Harata N (2002) Circadian rhythm in intracellular Cl^- activity of acutely dissociated neurons of suprachiasmatic nucleus. Am J Physiol Cell Physiol 282:C366–C373.

Strübing C, Krapivinsky G, Krapivinsky L, Clapham DE (2001) TRPC1 and TRPC5 form a novel cation channel in mammalian brain. Neuron 29:645–655.

Teshima K, Kim SH, Allen CN (2003) Characterization of an apamine-sensitive potassium current in suprachiasmatic nucleus neurons. Neuroscience 120:65–73.

Tischkau SA, Weber ET, Abbott SM, Mitchell JW, Gillette MU (2003) Circadian clock-controlled regulation of cGMP-protein kinase G in the nocturnal domain. J Neurosci 23:7543–7550.

van den Top M, Buijs RM, Ruijter JM, Delagrange P, Spanswick D, Hermes ML (2001) Melatonin generates an outward potassium current in rat suprachiasmatic nucleus neurones in vitro independent of their circadian rhythm. Neuroscience 107:99–108.

Walsh IB, van den Berg RJ, Rietveld WJ (1995) Ionic currents in cultured rat suprachiasmatic neurons. Neuroscience 69:915–929.

Welsh DK, Logothetis DE, Meister M, Reppert SM (1995) Individual neurons dissociated from rat suprachiasmatic nucleus express independently phases circadian firing rhythms. Neuron 14:697–706.

(Accepted 23 June 2004)
(Available online 23 September 2004)